Allosteric, chiral-selective drug binding to DNA

Xiaogang Qu[†], John O. Trent[‡], Izabela Fokt[§], Waldemar Priebe[§¶], and Jonathan B. Chaires[†¶]

[†]Department of Biochemistry, University of Mississippi Medical Center, 2500 North State Street, Jackson, MS 39216-4505; [‡]J. G. Brown Cancer Center, Department of Medicine, University of Louisville, 529 South Jackson Street, Louisville, KY 40202; and [§]University of Texas, M. D. Anderson Cancer Center, 1515 Holcombe Boulevard, Box 60, Houston, TX 77030

Edited by Donald M. Crothers, Yale University, New Haven, CT, and approved August 10, 2000 (received for review May 15, 2000)

The binding interactions of (−)-daunorubicin (WP900), a newly synthesized enantiomer of the anticancer drug (+)-daunorubicin, with right- and left-handed DNA, have been studied quantitatively by equilibrium dialysis, fluorescence spectroscopy, and circular dichroism. (+)-Daunorubicin binds selectively to right-handed DNA, whereas the enantiomeric WP900 ligand binds selectively to left-handed DNA. Further, binding of the enantiomeric pair to DNA is clearly chirally selective, and each of the enantiomers was found to act as an allosteric effector of DNA conformation. Under solution conditions that initially favored the left-handed conformation of [poly(dGdC)]$_2$, (+)-daunorubicin allosterically converted the polynucleotide to a right-handed intercalated form. In contrast, under solution conditions that initially favored the right-handed conformation of [poly(dGdC)]$_2$, WP900 converted the polynucleotide to a left-handed form. Molecular dynamics studies by using the AMBER force field resulted in a stereochemically feasible model for the intercalation of WP900 into left-handed DNA. The chiral selectivity observed for the DNA binding of the daunorubicin/WP900 enantiomeric pair is far greater than the selectivity previously reported for a variety of chiral metal complexes. These results open a new avenue for the rational design of potential anticancer agents that target left-handed DNA.

molecular recognition | allostery | drug design | molecular dynamics

DNA is polymorphic and exists in a variety of distinct conformations (1, 2). Duplex DNA can adopt a variety of sequence-dependent secondary structures that range from the canonical right-handed B form through the left-handed Z conformation. Multistranded triplex and tetraplex structures are now known to exist. All of these unique conformations may play important functional roles in gene expression. Consequently, there is intense current interest in the design and synthesis of small molecules that selectively target specific DNA structures, to inhibit the biological function in which these particular structures participate (3–10).

Enantiomers of chiral metal complexes have attracted considerable attention as potential structural probes of DNA conformation. Norden and Tjerneld (11) first reported the preference of the Δ enantiomer of *Tris*(dipyridyl)Fe(II) for right-handed B-form DNA. The Barton laboratory subsequently developed an elaborate series of chiral metal complexes, some of which were reported to recognize specific DNA conformational features (for reviews, see refs. 12–14). A comprehensive review of the interaction of chiral metal complexes with DNA (15) indicated, however, that the structural selectivity of these agents is ambiguous in many cases.

We report here a dramatic and unambiguous example of structural selectivity in DNA binding for the naturally occurring anticancer agent (+)-daunorubicin and its novel (−)-enantiomer, WP900 (Fig. 1). The synthesis of WP900 proved to be demanding and required some 37 steps. We find that the daunorubicin/WP900 enantiomeric pair can discriminate between right- and left-handed DNA, and that each compound can act as an allosteric effector to convert DNA to a conformation that binds each ligand with higher affinity. The structural selectivities of daunorubicin and WP900 appear to be far greater than those reported to date for any chiral metal compound. To the best of our knowledge, there have been no other reports of a detailed investigation of DNA binding for an enantiomeric pair that does not involve a chiral metal complex.

Materials and Methods

Materials. Daunorubicin was obtained from Sigma and was used without further purification. The concentrations of daunorubicin solutions were determined by optical absorption at 480 nm by using ε_{480} = 11,500 $M^{-1}\cdot cm^{-1}$. Calf thymus DNA (lot no. 27-4562-02) was purchased from Amersham Pharmacia and was sonicated and purified as described earlier (16). [poly(dGdC)]$_2$ (lot no. 5067910021) was purchased from Amersham Pharmacia. All of the DNA samples were dialyzed into appropriate buffers for at least 24 h. DNA concentrations were determined by UV absorption by using molar ε_{260} = 12,824 $M^{-1}\cdot cm^{-1}$ and ε_{254} = 16,800 $M^{-1}\cdot cm^{-1}$ for calf thymus DNA and [poly(dGdC)]$_2$, respectively.

Synthesis of WP900. Synthesis of WP900, a left-handed (−)-enantiomer of the natural product (+)-daunorubicin, was achieved by multistep synthesis of an aglycon (−)-daunomycinone and the sugar moiety D-daunosamine, daunorubicin's two optically active components, and their subsequent stereoselective coupling. The aglycon (−)-daunomycinone with 7*R*,9*R* configuration was prepared by using a modification of the Swenton method (17), whereas D-daunosamine was synthesized from D-galactose. Full details of the synthesis will be published elsewhere.

Both (−)-daunomycinone and 4-*O*-acetyl-1-*O*-*t*-butyldimethylsilyl-3-*N*-trifluroacetamido-D-daunosamine had [^{1}H]NMR characteristics and optical rotation that agree with the data reported for natural daunomycinone and the analogously protected L-daunosamine derivative. For the coupling reaction, 4-*O*-acetyl-1-*O*-*t*-butyldimethylsilyl-3-*N*-trifluoroacetamido-D-daunosamine was reacted with trimethylsilyl bromide to generate the glycosyl donor 4-*O*-acetyl-3-*N*-trifluoroacetamido-D-daunosaminyl bromide. Subsequent coupling with (−)-daunomycinone was carried out in CH_2Cl_2 solution in the presence of HgO and $HgBr_2$ to give the α anomer as a major product. In a two-step deblocking procedure, the 4′-*O*-acetyl and *N*-trifluoroacetyl protecting groups were removed by using NaOMe in MeOH and 1 M NaOH, respectively. The final product (−)-daunorubicin (WP900) was purified as a free base by column chromatography on silica gel 60 (EM Merck) by using $CHCl_3$, $CHCl_3$/MeOH (98:2 vol/vol), and $CHCl_3$/MeOH (95:5 vol/vol) as eluents. The purified WP900 was converted to the hydrochloride by treatment with 1 M methanolic HCl solution and precipitation with diethyl ether. The composition of the product WP900 was confirmed by [^{1}H]NMR and elemental analysis. The

This paper was submitted directly (Track II) to the PNAS office.

Abbreviation: CD, circular dichroism.

See commentary on page 11685.

¶Address reprint requests to either author. E-mail: jchaires@biochem.umsmed.edu or wp@wt.net.

The publication costs of this article were defrayed in part by page charge payment. This article must therefore be hereby marked "*advertisement*" in accordance with 18 U.S.C. §1734 solely to indicate this fact.

Article published online before print: *Proc. Natl. Acad. Sci. USA*, 10.1073/pnas.200221397. Article and publication date are at www.pnas.org/cgi/doi/10.1073/pnas.200221397

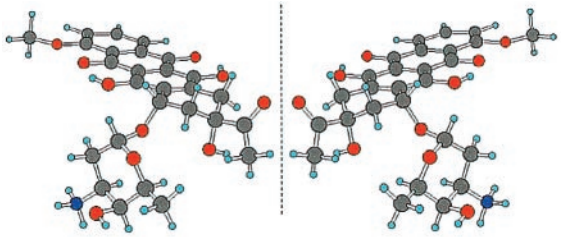

Fig. 1. Structures of (+)-daunorubicin (*Left*) and (−)-daunorubicin, WP900 (*Right*).

measured optical rotation for WP900 was $[\alpha]_D^{20} = -251 \pm 4°$ (c = 0.09, MeOH), whereas the reported optical rotation of (+)-daunorubicin was $+248 \pm 5°$ (c = 0.1, MeOH) (18).

Instrumentation. Absorbance spectra were recorded by using a Cary–Varian (Palo Alto, CA) 3E UV–visible spectrophotometer with 1-cm cells. Fluorescence data were recorded by using I.S.S. (Champaign, IL) Greg 200 fluorometer with excitation at 480 nm, and emission fluorescence was monitored from 500 to 700 nm. Circular dichroism studies were recorded at 20°C on a Jasco (Easton, MD) J500A spectropolarimeter.

Binding Studies. Daunorubicin and WP900 binding to calf thymus DNA or $[poly(dGdC)]_2$ was measured by fluorescence titration by using protocols developed in this laboratory (19). When required, binding isotherms were fit to Crothers's allosteric model (20) by an iterative process as described previously (21).

Dialysis. Samples of $[poly(dGdC)]_2$ were separately equilibrated to 0.2 M and 3 M NaCl by dialysis and adjusted to a concentration of 100 μM by dilution with the appropriate dialysate. Under these conditions, $[poly(dGdC)]_2$ retains the B conformation in 0.2 M NaCl and adopts the Z conformation in 3 M NaCl buffered solution. One-milliliter volumes of B- or Z-form $[poly(dGdC)]_2$ were then dialyzed against a 10-ml solution containing a 1:1 mixture of daunorubicin and WP900. After 24 h dialysis, circular dichroism (CD) spectra of the dialysate solutions were measured to determine the enrichment of particular enantiomeric forms.

Molecular Modeling. The starting model for daunorubicin was taken from the literature (22) and was inverted to create the WP900 enantiomer. Parameterization and partial charges were obtained from *ab initio* calculations at the 6–31G* level with the GAMESS (23) package; the restrained electrostatic potential fit routine (24, 25) was used. The geometry of the resulting daunorubicin closely resembled the published crystal structure. The starting models for the right-handed B and left-handed Z forms of $d(CGC\mathbf{GC}GCG)_2$ were created by using the standard conformations provided in the MACROMODEL program (26). The intercalation site (highlighted in bold) for the right-handed form was built by inserting standard B-form phosphate backbone intercalation site conformations (22). The Z-DNA intercalation site was built from the Z form of $d(CGC\mathbf{GC}GCG)_2$ by separating the bases highlighted in bold by 6.8 Å, with reduction of the helical twist and adjustment of the phosphate backbone angles. The geometry of the constructed Z-DNA intercalation site was optimized before docking of the intercalator. Daunorubicin and WP900 ligand molecules were then inserted into the generated intercalation sites by superimposing the DNA–daunorubicin crystal structure. Four models were used for simulations: daunorubicin and WP900 each bound to the B-form intercalation site, and daunorubicin and WP900 each bound to the corresponding Z-form intercalation site. The intercalation sites were optimized by molecular mechanics and dynamics with restraints of 100 kcal·(mol·Å)$^{-1}$ applied to the non-intercalation site bases by using the implicit solvation within MACROMODEL. The optimal positioning of each intercalator was determined by a grid search with translation of 8 × 8 Å and rotation ± 90° (using 1-Å and 15° resolution steps). The resulting structures were used as starting structures for the explicit solvation calculations.

The model structures were hydrated by using standard AMBER 5.0 (27) rules in a 10-E box of TIP3P waters. Sodium cations for the B-form complexes were added by using the EDIT placement routine, and chloride anions were added randomly for charge neutrality. The Na^+ and Cl^- counterions for the Z-form complexes were added randomly to simulate a neutral 3-M aqueous NaCl solution.

The systems were heated slowly to 300 K and equilibrated carefully during 50 ps with gradual decrease of restraints on the DNA and ligand from 100 to 10 kcal·(mol·Å)$^{-1}$. Further 400-ps and 600-ps periods of restrained molecular dynamics were used for the B-form and Z-form complexes, respectively, to ensure complete solvent equilibrium. Molecular dynamics simulations by using the AMBER-95 force field were performed in the isothermal isobaric ensemble (P = 1 atm, T = 300 K) with the AMBER 5.0 program (27), using periodic boundary conditions and the Particle-Mesh-Ewald algorithm. A 2-fs time step was used with all bond distances frozen by using SHAKE. After heating and equilibration, molecular dynamics production runs of 800 ps were used to derive average structures for the complexes taken from 50 snapshots accumulated in the last 50 ps with subsequent minimization.

Results and Analysis

Structural Selectivity of Daunorubicin and WP900. Fig. 2 shows the results of dialysis experiments designed to reveal the structural selectivity of daunorubicin enantiomers. A racemic mixture of daunorubicin and WP900 was prepared by mixing equimolar amounts of the pure enantiomers (Fig. 2*A*). The racemic mixture was dialyzed against either B- or Z-form $[poly(dGdC)]_2$, and circular dichroism was used to monitor the dialysate for enrichment in the enantiomer with poorer affinity for the DNA conformation contained within the dialysis tube. Under solution conditions that favor B-form $[poly(dGdC)]_2$, the dialysate was enriched in WP900 (Fig. 2*B*, curve a). This result indicates unambiguously that daunorubicin binds preferentially to right-handed DNA compared with WP900. In contrast, under solution conditions that favored Z-form $[poly(dGdC)]_2$, the dialysate was enriched in daunorubicin, indicating that WP900 binds preferentially to left-handed DNA (Fig. 2*B*, curve b). Binding of daunorubicin and WP900 to DNA is both structurally and chirally selective.

Binding Constants for the Interaction of Daunorubicin and WP900 with DNA. Table 1 shows the structural selectivity of daunorubicin and WP900 more quantitatively. Binding constants were measured by fluorescence titration methods, in which fixed concentrations of either daunorubicin or WP900 were titrated with increasing DNA concentrations (see Fig. 5, which is published as supplemental data on the PNAS web site, www.pnas.org). In this protocol, the chemical potential of the drug is not sufficiently high to allosterically alter the DNA conformation, and binding constants measure the strength of binding to the particular DNA form stable under the conditions of the experiment. Table 1 shows that, under identical conditions, daunorubicin binds to right-handed calf thymus DNA 24-fold more tightly than does WP900. Similarly, in 0.2-M NaCl solutions that favor the right-handed form of $[poly(dGdC)]_2$, daunorubicin binding is 21-fold tighter than WP900. In contrast, in 3-M NaCl, where left-handed $[poly(dGdC)]_2$ is favored, the WP900 binding constant is 5.0-fold greater than that measured for daunorubicin. These results

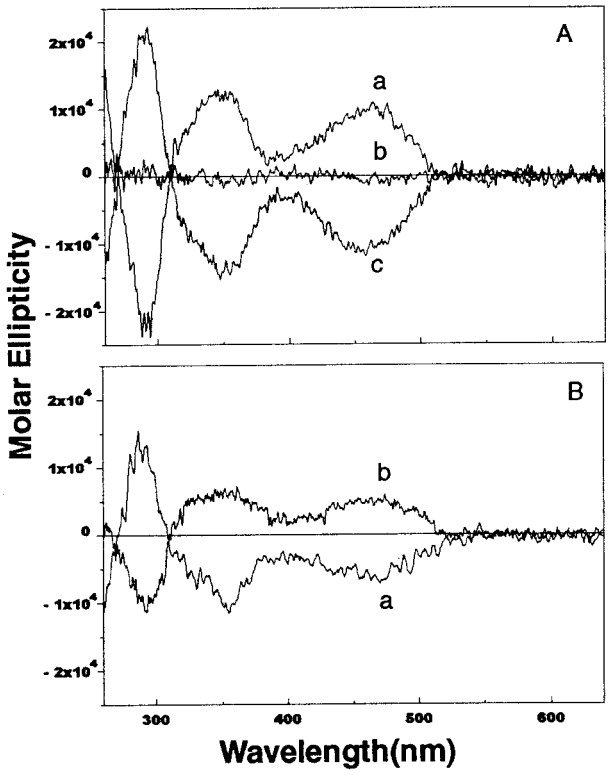

Fig. 2. CD spectra of daunorubicin and WP900 solutions. (*A*) Curve a, daunorubicin; curve c, WP900; curve b, a 1:1 molar ratio mixture of daunorubicin and WP900. (*B*) Curve a, CD spectrum of the dialysate after dialysis of the racemic mixture against B-form [poly(dGdC)]$_2$ in 0.2 M NaCl. The dialysate is enriched in WP900, indicating preferential binding of daunorubicin to the right-handed DNA. Curve b, CD spectrum of the dialysate after dialysis of the racemic mixture against Z-form [poly(dGdC)]$_2$ in 3.0 M NaCl. The dialysate is enriched in daunorubicin, indicating preferential binding of WP900 to the left-handed DNA. Details of the competition dialysis procedure are described in *Materials and Methods*.

quantitatively confirm the qualitative structural selectivity evident in the results shown in Fig. 2.

Allosteric Conversion of DNA by Daunorubicin and WP900. Daunorubicin is known to allosterically convert Z-DNA to an intercalated right-handed form (21). Fig. 3 shows the results of an experiment designed to qualitatively demonstrate allosteric binding of daunorubicin and WP900 to DNA. A sample solution of [poly(dGdC)]$_2$ was equilibrated to 2.25 M NaCl, a salt concentration near the midpoint of the B–Z transition (21). Under such conditions, the solution contains a mixed population of B and Z forms and yields a CD spectrum reflecting that mixture (Fig. 3, curve a). If daunorubicin is added to that solution (2 μM final concentration), the CD spectrum changes to one characteristic of right-handed DNA (Fig. 3, curve b).

Table 1. Binding constants for the interactions of (+)-daunorubicin or (−)-daunorubicin (WP900) with B- and Z-form DNA

		$K/10^4$ M^{-1}	
DNA	[Na$^+$], M	Daunorubicin	WP900
Calf thymus DNA	0.2	19.6 ± 3.0	0.8 ± 0.1
B-form [poly(dGdC)]$_2$	0.2	25.7 ± 2.0	1.2 ± 0.3
Z-form [poly(dGdC)]$_2$	3.0	0.2 ± 0.1	1.0 ± 0.2

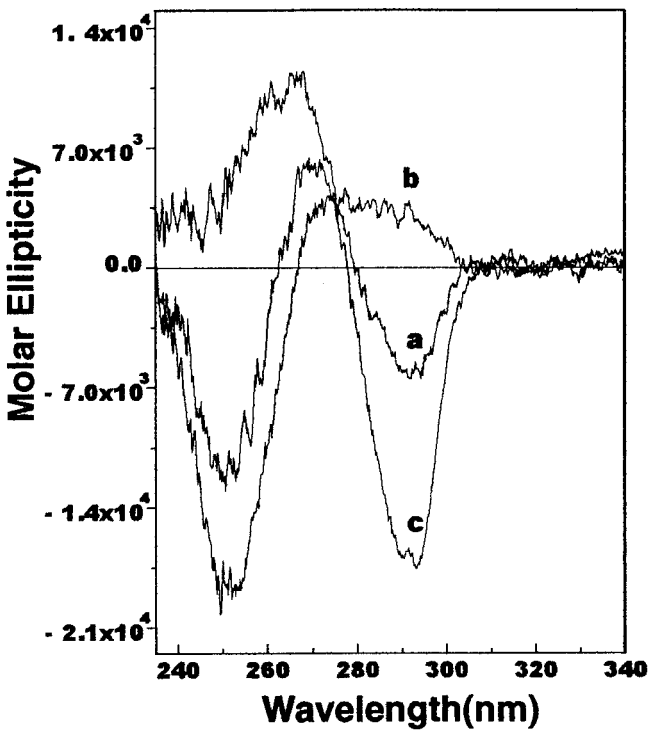

Fig. 3. CD spectra of [poly(dGdC)]$_2$ at 100 μM (bp) in buffered aqueous solution containing 2.25 M NaCl. Curve a, the DNA alone, showing a spectrum characteristic of a mixture of B- and Z-form conformations. Curve b, the DNA with daunorubicin added to a final concentration of 2 μM. The molar ratio of drug:bp is 0.02. The resultant spectrum is characteristic of right-handed DNA. Curve c, the DNA with WP900 added to a final concentration of 3 μM. The molar ratio of drug:bp is 0.03. The resultant spectrum is characteristic of left-handed DNA.

Addition of daunorubicin allosterically shifts the B-to-Z equilibrium to favor the right-handed B-form. In contrast, if WP900 (3 μM) is added to the 2.25-M NaCl [poly(dGdC)]$_2$ solution, the CD spectrum changes to one characteristic of left-handed Z-DNA (Fig. 3, curve c). These results show that daunorubicin and WP900 not only can bind selectively to right- or left-handed DNA, but also can drive the allosteric conversion of DNA to the chiral form preferred by each ligand.

Quantitative Analysis of the Cooperative DNA Binding of Daunorubicin and WP900. Binding isotherms for the interaction of daunorubicin and WP900 with both B- and Z-form DNA were obtained by using a titration protocol in which the total DNA concentration remained constant while the total drug concentration was increased (21) (Figure 6, Supplementary Material). These isotherms revealed in some cases pronounced positive cooperativity that was interpreted as arising from the coupling of binding to a conformational transition of the polynucleotide to the higher affinity form (20, 21). First, daunorubicin bound to B-form [poly(dGdC)]$_2$ in 2.1 M NaCl with no apparent positive cooperativity (Fig. 6*A*, Supplemental Material). Data were fit to a simple neighbor-exclusion model (28, 29) to yield a binding constant of 9.0×10^5 M^{-1} and a neighbor exclusion parameter of 2.3 (Table 3, Supplementary Materials). In contrast, daunorubicin bound to Z-form [poly(dGdC)]$_2$ in 3.0 M NaCl with clear positive cooperativity (Fig. 6*A*, Supplementary Material). These data were analyzed by using Crothers' allosteric binding model (20), yielding the fitted parameters listed in Table 2. The most important conclusion derived from the quantitative data in Table 2 was that daunorubicin strongly prefers binding to the

Table 2. Summary of the parameters describing the allosteric binding of (+)-daunorubicin and (−)-daunorubicin (WP900) to [poly(dGdC)]$_2$ under ionic conditions favorable to either the Z- or B-DNA conformation

Parameter*	Daunorubicin† Z → B	WP900‡ B → Z
σ	0.001	0.01
s	0.635	0.92
K_1	0.8×10^4	1.5×10^4
K_2	3.5×10^5	7.8×10^4
K_2/K_1	44	5.2

*The parameter, σ, is the nucleation parameter for the conversion of a base pair within a stretch of Z (or B) helix to the B (or Z) conformation; s is the equilibrium constant for the conversion of a base pair at a pre-existing B-Z interface from the Z (or B) to the B (or Z) conformation; and K_1 is the binding constant for the interaction of a drug molecule with an isolated site in the form-1 conformation; K_2 is the binding constant for the interaction of a drug molecule with an isolated site in the form-2 conformation.

†Daunorubicin binding to [poly(dGdC)]$_2$ in buffered 3.0 M NaCl solution. Titration experiments were carried out using the same conditions described in supplementary Table 3. In this case, K_1 refers to binding to the initial Z-form DNA, whereas K_2 refers to binding to the preferred B-form DNA.

‡WP900 binding to [poly(dGdC)]$_2$ in buffered 2.1 M NaCl solution. Titration experiments were carried out using the same conditions described in supplementary Table 3. In this case, K_1 refers to binding to the initial B-form DNA, whereas K_2 refers to binding to the preferred Z-form DNA.

right-handed form of [poly(dGdC)]$_2$, and allosterically converts the initial Z-form to the more favorable right-handed conformation. The ratio of daunorubicin binding constants for the B- and Z-forms is 44 (Table 2), and it is this difference in binding affinity that drives the allosteric conversion.

The binding behavior is completely reversed for the enantiomer WP900. In contrast to the noncooperative binding observed for interaction of daunorubicin with B-form [poly(dGdC)]$_2$ in 2.1 M NaCl, WP900 binds with pronounced positive cooperativity under the same conditions (Fig. 6*B*, Supplementary Material). Fits to the allosteric binding model yielded the parameters listed in Table 2. In this case, WP900 facilitates the B-to-Z transition in the lower NaCl concentration that would otherwise favor the right-handed polynucleotide conformation. The ratio of WP900 binding constants to the Z- and B-form is 5.2, and this affinity difference drives the allosteric conversion of the polynucleotide. Finally, WP900 binds to Z-form [poly(dGdC)]$_2$ in 3.0 M NaCl with no apparent positive cooperativity (Fig. 6*B*, Supplementary Material). These data were fit to a simple neighbor-exclusion model to yield a binding constant of 0.66×10^5 M^{-1} and a neighbor exclusion parameter of 1.7 (Table 3, Supplementary Materials).

The quantitative analyses of these binding data are fully consistent with the qualitative behavior shown in Fig. 3. The important conclusion from these studies is that both daunorubicin and WP900 not only can selectively recognize right- and left-handed DNA, respectively, but they both also can act as allosteric effectors to drive a DNA conformational transition to the forms that bind each ligand with higher affinity.

Structural Basis of Selectivity. The strong preference of daunorubicin for right-handed, B-form DNA is thought to arise from the precise fit of the daunosamine moiety into the minor groove (21). High-resolution crystal structures of daunorubicin complexed to DNA show that the angle of the daunosamine relative to the intercalated chromophore is such that it aligns with the minor groove, allowing a favorable stereochemical fit (22). Because there are no crystal structures of WP900 bound to Z-DNA, computer simulations by using molecular dynamics were used to build a reasonable model of the complex. Fig. 4 shows WP900 intercalated into left-handed DNA. The model in Fig. 4 is energetically and stereochemically feasible and provides a detailed view of a left-handed DNA intercalation complex. Simulations of all possible combinations of daunorubicin enantiomers and DNA forms yielded only two stable complexes, one with daunorubicin bound to B-form DNA and another with WP900 bound to Z-form DNA. The B-form DNA–WP900 and Z-form DNA–daunorubicin complexes were not stable and resulted in disruption of duplex stability and loss of intercalation. The instability of these complexes may contribute to the allosteric effect by facilitating conformational changes in the duplex backbone. The simulated B-form DNA–daunorubicin complex (not shown) resembles the published crystal structure (22). The Z-form DNA–WP900 complex (Fig. 4) shows that the AMBER-95 force field is able to reproduce the left-handed DNA, as the structure is conserved under the salt conditions used, and that the intercalation complex is stable. The models reproduce the experimental observations of WP900 preferentially binding to Z-form DNA and daunorubicin preferentially binding to B-form DNA. The preference of WP900 for Z-form DNA arises from the orientation and shape complementarity of the D-daunosamine with the minor groove. In contrast, the L-daunosamine group of daunorubicin has steric clashes with the minor groove and backbone of Z-DNA, which causes a positional change of the intercalated chromophore that decreases the overall integrity of the binding site. Analogous effects are observed for WP900 and the disfavored B-form DNA. We emphasize that the allosteric conversions of the B- to the Z-form

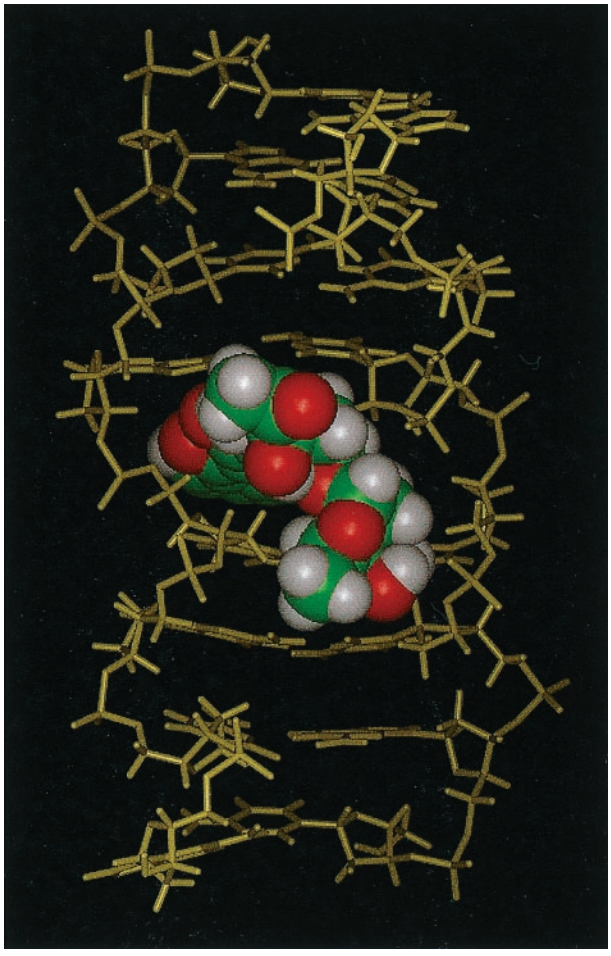

Fig. 4. Energy-minimized average model of the left-handed Z-DNA–WP900 intercalation complex formed with the d(CGCGCGCG)$_2$ duplex (see text).

or of the Z- to the B-form were not observed in our simulations, even in runs up to 5 ns. Because the experimental time scale for these allosteric conversions is on the order of minutes, we would in fact not expect to see such behavior in the time scales used in our simulations. (Plots of the trajectories of bond angles in the residues within Z DNA intercalation site are provided in Supplementary Materials, Figs. 7–10).

Discussion

We report here biophysical studies of the binding interactions of daunorubicin and its (−)-enantiomer WP900 with DNA. The results provide a striking example of chiral-selective recognition of DNA. WP900 binds to DNA with unique structural selectivity and strongly prefers left-handed DNA to the normal right-handed B-form, in contrast to daunorubicin, for which the pattern of selectivity is reversed. Molecular dynamics simulations show that intercalation into left-handed Z-DNA represents a plausible mode of WP900 binding.

Earlier detailed studies of the highly cooperative binding of common intercalators to left-handed Z-DNA revealed that these compounds strongly prefer the right-handed duplex conformation. Ethidium and actinomycin D bind 300-fold and 1000-fold more tightly to B- rather than Z-DNA, respectively (30, 31), whereas daunorubicin binds 30-fold more tightly to the B-form DNA (21). These early studies provided the first indications of a structural selectivity for intercalator ligands. Because there were no enantiomers available at the time for these compounds, it was not possible to study their selectivity toward Z-DNA, a situation that has been remedied with the synthesis of WP900.

Part of the initial excitement over chiral metal complexes was their potential to discriminate between right- and left-handed DNA (12, 13). One of the earliest compounds that emerged from the Barton laboratory was *Tris*-(phenanthroline)Ru(II). The chiral selectivity of this compound was admitted to be weak (12, 13), at best, and more quantitative studies later revealed that there in fact was no appreciable stereoselective DNA binding of the isomers of *Tris*-(phenanthroline)Ru(II) (32, 33). Enantiomers of *Tris*-(4,7 diphenylphenanthroline)Ru(II) showed apparently improved selectivity (34). It was reported that the Δ-enantiomer bound selectively to B-DNA, whereas the affinity of the Λ-enantiomer for B-DNA was negligible. However both the Δ and Λ isomers bound to Z-form DNA with comparable affinity. The enantiomers of *Tris*-(4,7 diphenylphenanthroline)-Ru(II) could thus potentially probe for B-type DNA, but could only indirectly probe for the Z form. The behavior reported here for the anthracycline enantiomers stands in sharp contrast to this earlier work. In the present case, the binding to B- and Z-DNA by daunorubicin and WP900 is mutually complementary. Daunorubicin binds well to B-DNA but not to Z-DNA, whereas WP900 binds selectively to Z-DNA over B-DNA. In each case, enantiomer selectivity is sufficiently strong to drive the allosteric conversion of DNA to the preferred conformation. Whereas certain chiral metal complexes convert Z-DNA to the B form (32), none were ever reported to convert B-DNA to the Z form, as does WP900. The failure of any of the chiral metal complexes to convert right-handed DNA to a left-handed form is a consequence of their relatively poor structural selectivity for the Z conformation. Chiral metal complexes have failed to become widespread or reliable probes of DNA conformation despite their early promise. A comprehensive and critical review of the DNA binding of chiral metal complexes (15) documented ambiguities in their structural selectivity and concluded in part that metal complexes may recognize sites that are easily distorted rather than recognizing unusual structures *per se*.

Our data show clearly that WP900 binds preferentially to left-handed Z-DNA, although we caution that we cannot yet identify its binding mode with certainty. Determination of the binding mode is a difficult task in the absence of high-resolution structural data (35). Hydrodynamic methods (viscosity, sedimentation) that are normally used as criteria for the binding mode are difficult to apply to Z-DNA because of the high-salt solutions required to maintain the structure, and because of a poorly defined theoretical basis for interpreting data for the Z-DNA geometry. Intercalation of WP900 into Z-DNA is the likely binding mode, a supposition that is supported by our computer simulations by using molecular dynamics (Fig. 4), where a stereochemically reasonable WP900-Z-DNA intercalation complex can be formed. Because the same methods accurately reproduce the structure of the B-DNA–daunorubicin intercalation complex, for which high-resolution x-ray data are available, the model derived from molecular dynamics is plausible. We note that a variety of computer simulations have previously been performed in attempts to obtain models for a Z-DNA intercalation complex (36, 37). The methods used in our studies are decided improvements over these earlier attempts for several reasons. First, a greatly improved AMBER force field with the Particle-Mesh Ewald summation method has been used. Second, our simulations include both solvent and ions, whereas earlier studies modeled structures *in vacuo*. Finally, reliable high-resolution structural data for our system were available as starting models for at least the B family of structures used in our simulations. The average structure obtained from the molecular dynamics simulation for the daunorubicin-B-DNA intercalation complex is consistent with and essentially reproduces existing structural data (22). The Z-DNA simulations are similarly in close agreement with existing structural data for Z-DNA for the nonintercalated region of the complex. No structural data exist for a Z-DNA intercalation complex. Page limitations prohibit a detailed description of all of the results from dynamic DNA–ligand simulations that were conducted; full details of the extensive studies will be described elsewhere.

Z-DNA is not a mirror image structure of B-DNA, so we do not expect exact symmetry in the magnitudes of the binding constants for daunorubicin and WP900 shown in Table 1, as is in fact the case. It is also necessary to consider difference in salt concentrations when considering the binding constants presented in Tables 1 and 2. For example, at first glance, the binding constants for the interactions of WP900 with B- and Z-form $[poly\ (dGdC)]_2$ appear to be similar. But the binding constants refer to 0.2 and 3.0 M NaCl, and direct comparison requires correction for the well-known salt dependence of the binding constant for charged intercalators. Determination of the binding constants for the two DNA conformations is a feature of the allosteric model, and the ratio of the binding constants K_2/K_1 shown in Table 2 provides a direct measure of the relative binding affinities for B- and Z-DNA under the same solution conditions.

The biological function of Z-DNA remains poorly defined but is an area of active research (38–41). What is clear at this point is that sequences with Z-forming potential are nonrandomly distributed throughout the human genome, and that there are certain eukaryotic proteins that bind specifically to Z-DNA (42–44). Z-DNA forms in the wake of RNA polymerase as it transcribes DNA (45). The most thoroughly characterized Z-DNA binding protein to date is the RNA-editing enzyme double-stranded RNA adenosine deaminase (46–50), whose Z-DNA binding activity may serve to localize it to transcriptionally active regions of the genome where it may then exercise its RNA editing function (39). Z-DNA has been demonstrated to be present in the transcriptional regulatory regions of the *c-myc* gene (41). Whereas our intent in these fundamental studies was to study basic aspects of DNA molecular recognition, WP900 could prove to be useful as a probe of Z-DNA regions in the genome, or as an inhibitor of as yet unidentified biological functions that may depend on Z-DNA. Preliminary cytotoxicity studies show that WP900 is indeed biologically active. *In vitro*

cytotoxicity was measured by using human carcinoma cell lines KB3.1 (sensitive) and KB-V1 (multidrug resistant). The ID_{50} values by using the KB3.1 sensitive cell line were 8.3 ($\pm$ 3.0) and 0.4 ($\pm$0.1) μM for WP900 and doxorubicin, respectively. The ID_{50} values by using the KB-V1 multidrug resistant cell line were 19 ($\pm$ 9) and $>$100 μM for WP900 and doxorubicin, respectively. WP900 is not as cytotoxic against sensitive cells as is doxorubicin, but is far more active against multidrug-resistant cells. These preliminary data suggest that WP900 may act by a mechanism distinct from the topoisomerase II inhibition normally attributed to the anthracyclines. More detailed biological studies to clarify WP900's mechanism of action are clearly needed.

We thank Professor Terry Jenkins (University of Bradford, U.K.), Dr. David Dignam (Medical College of Ohio), and Dr. Loren Williams (Georgia Institute of Technology) for helpful comments on the manuscript. We thank Dr. Daquan Gao for the preparation of the trajectory plots presented in Supplementary Materials. This work was supported by Grants CA35635 (to J.B.C.) and CA50270 (to W.P.) from the National Cancer Institute and by Grant ATP 15-090 (to W.P.) from the Texas Higher Education Coordinating Board.

1. Sinden, R. R. (1994) *DNA Structure and Function* (Academic, San Diego).
2. Neidle, S. (1999) *Oxford Handbook of Nucleic Acid Structure* (Oxford Univ. Press, New York).
3. Hurley, L. H. & Boyd, F. L. (1988) *Trends Pharmacol. Sci.* **9,** 402–407.
4. Hurley, L. H. (1989) *J. Med. Chem.* **32,** 2027–2033.
5. Mergny, J. L., Duval-Valentin, G., Nguyen, C. H., Perrouault, L., Faucon, B., Rougee, M., Montenay-Garestier, T., Bisagni, E. & Helene, C. (1992) *Science* **256,** 1681–1684.
6. Mergny, J. L. & Helene, C. (1998) *Nat. Med.* **4,** 1366–1367.
7. Chaires, J. B. (2000) *Curr. Med. Chem.* **7,** 1–115.
8. Chaires, J. B. (1996) *Advances in DNA Sequence Specific Agents* (JAI Press, Greenwich, CT).
9. Perry, P. J. & Jenkins, T. C. (1999) *Exp. Opin. Invest. Drugs* **8,** 1981–2008.
10. Jenkins, T. C. (2000) *Curr. Med. Chem.* **7,** 99–115.
11. Norden, B. & Tjerneld, F. (1976) *FEBS Lett.* **67,** 368–370.
12. Barton, J. K. (1986) *Science* **233,** 727–734.
13. Barton, J. K. (1983) *J. Biomol. Struct. Dyn.* **1,** 621–632.
14. Chow, C. S. & Barton, J. K. (1992) *Methods Enzymol.* **212,** 219–242.
15. Norden, B., Lincoln, P., Akerman, B. & Tuite, E. (1996) *Met. Ions Biol. Syst.* **33,** 177–252.
16. Chaires, J. B., Dattagupta, N. & Crothers, D. M. (1982) *Biochemistry* **21,** 3933–3940.
17. Swenton, J. S., Freskos, J. N., Morrow, G. W. & Sercel, A. D. (1984) *Tetrahedron* **40,** 4625–4632.
18. Budavari, S., O'Neil, M. J., Smith, A. & Heckelman, P. E., eds. (1989) *The Merck Index* (Merck, Rahway, NJ), 11th Ed., p. 445.
19. Qu, X. & Chaires, J. B. (1999) in *Methods in Enzymology*, eds. Johnson, M. L. & Brand, L. (Academic, San Diego), Vol. 321, pp. 353–369.
20. Dattagupta, N., Hogan, M. & Crothers, D. M. (1980) *Biochemistry* **19,** 5998–6005.
21. Chaires, J. B. (1986) *J. Biol. Chem.* **261,** 8899–8907.
22. Wang, A. H., Ughetto, G., Quigley, G. J. & Rich, A. (1987) *Biochemistry* **26,** 1152–1163.
23. Schmidt, M. W., Baldridge, K. K., Boatz, J. A., Elbert, S. T., Gordon, M. S., Jensen, J. J., Koseki, S., Matsunaga, N., Nguyen, K. A., Su, S., *et al.* (1993) *J. Comput. Chem.* **14,** 1347–1363.
24. Bayly, C. I., Cieplak, P., Cornell, W. D. & Kollman, P. A. (1993) *J. Phys. Chem.* **97,** 10269–10280.
25. Cornell, W. D., Cieplak, P., Bayly, C. I. & Kollman, P. A. (1993) *J. Am. Chem. Soc.* **115,** 9620–9631.
26. Mohamadi, F., Richards, N. G., Guida, W. C., Liskamp, R., Lipton, M., Caufield, C., Chang, G., Hendricksen, T. & Still, W. C. (1990) *J. Comput. Chem.* **11,** 440–455.
27. Cornell, W. D., Cieplak, P., Bayly, C. I., Gold, I. R., Merz, K. M., Ferguson, D. M., Spellmeyer, D. C., Fox, F., Caldwell, J. W. & Kollman, P. A. (1995) *J. Am. Chem. Soc.* **117,** 5179–5197.
28. McGhee, J. D. & Hippel, P. H. von (1974) *J. Mol. Biol.* **86,** 469–489.
29. Correia, J. J. & Chaires, J. B. (1994) *Methods Enzymol.* **240,** 593–614.
30. Walker, G. T., Stone, M. P. & Krugh, T. R. (1985) *Biochemistry* **24,** 7462–7471.
31. Walker, G. T., Stone, M. P. & Krugh, T. R. (1985) *Biochemistry* **24,** 7471–7479.
32. Hard, T., Hiort, C. & Norden, B. (1987) *J. Biomol. Struct. Dyn.* **5,** 89–96.
33. Satyanarayana, S., Dabrowiak, J. C. & Chaires, J. B. (1993) *Biochemistry* **32,** 2573–2584.
34. Barton, J. K., Basile, L. A., Danishefsky, A. & Alexandrescu, A. (1984) *Proc. Natl. Acad. Sci. USA* **81,** 1961–1965.
35. Suh, D. & Chaires, J. B. (1995) *Bioorg. Med. Chem.* **3,** 723–728.
36. Prabhakaran, M. & Harvey, S. C. (1988) *Biopolymers* **27,** 1239–1248.
37. Gupta, G., Dhingra, M. M. & Sarma, R. H. (1983) *J. Biomol. Struct. Dyn.* **1,** 97–113.
38. Herbert, A. & Rich, A. (1996) *J. Biol. Chem.* **271,** 11595–11598.
39. Herbert, A. & Rich, A. (1999) *Genetica (The Hague)* **106,** 37–47.
40. Gagna, C. E., Kuo, H. & Lambert, W. C. (1999) *Cell Biol. Int.* **23,** 1–5.
41. Kuramoto, N., Ogita, K. & Yoneda, Y. (1999) *Jpn. J. Pharmacol.* **80,** 103–109.
42. Gohlke, C., Murchie, A. I., Lilley, D. M. & Clegg, R. M. (1994) *Proc. Natl. Acad. Sci. USA* **91,** 11660–11664.
43. Arndt-Jovin, D. J., Udvardy, A., Garner, M. M., Ritter, S. & Jovin, T. M. (1993) *Biochemistry* **32,** 4862–4872.
44. Bechert, T., Diekmann, S. & Arndt-Jovin, D. J. (1994) *J. Biomol. Struct. Dyn.* **12,** 605–623.
45. Liu, L. F. & Wang, J. C. (1987) *Proc. Natl. Acad. Sci. USA* **84,** 7024–7027.
46. Berger, I., Winston, W., Manoharan, R., Schwartz, T., Alfken, J., Kim, Y. G., Lowenhaupt, K., Herbert, A. & Rich, A. (1998) *Biochemistry* **37,** 13313–13321.
47. Herbert, A., Lowenhaupt, K., Spitzner, J. & Rich, A. (1995) *Proc. Natl. Acad. Sci. USA* **92,** 7550–7554.
48. Herbert, A., Lowenhaupt, K., Spitzner, J. & Rich, A. (1995) *Nucleic Acids Symp. Ser.* **33,** 16–19.
49. Schade, M., Turner, C. J., Kuhne, R., Schmieder, P., Lowenhaupt, K., Herbert, A., Rich, A. & Oschkinat, H. (1999) *Proc. Natl. Acad. Sci. USA* **96,** 12465–12470.
50. Schwartz, T., Rould, M. A., Lowenhaupt, K., Herbert, A. & Rich, A. (1999) *Science* **284,** 1841–1845.